Elastic constants and specific-heat measurements on single crystals of La_2CuO_4

A. Migliori, William M. Visscher, S. E. Brown, Z. Fisk, S.-W. Cheong, B. Alten, E. T. Ahrens, and K. A. Kubat-Martin
Los Alamos National Laboratory, Los Alamos, New Mexico 87545

J. D. Maynard, Y. Huang, D. R. Kirk, K. A. Gillis, H. K. Kim, and M. H. W. Chan
Department of Physics, The Pennsylvania State University, University Park, Pennsylvania 16802
(Received 10 July 1989)

We measured all nine elastic constants of a nonsuperconducting single crystal of La_2CuO_4 at 310, 297, and 44 K using a small-sample resonant ultrasound technique. Weak features in resonant frequencies dependent on compressional moduli were observed near 29 K, and a broad minimum occurred at 38 K, near the superconducting transition temperature of optimally doped La_2CuO_4. The features are also reflected in the specific heat.

Since the discovery of the high-temperature superconducting oxides, there has been considerable effort devoted to determining the mechanism responsible for the high transition temperatures. To develop an understanding of the intrinsic properties of these systems, it is often preferable to measure single-crystal bulk samples. This is particularly true for transport and ultrasound measurements, as these are capable of probing the strong anisotropy present.

In this paper, we report measurements on an untwinned single crystal of La_2CuO_4 using a new small-sample resonant ultrasound technique, and we have complemented the results with ac heat-capacity measurements. We have made the first determination of all nine independent elastic constants of this orthorhombic material at several temperatures, and, for our nonsuperconducting stoichiometric crystal, we have observed weak features in the compressional moduli and heat capacity near 29 K, and a broader feature at 38 K, near the transition temperature T_c of the optimally doped superconducting material.

The presence of features in the elastic constants near T_c may be important to the theory of the high-temperature oxide superconductors. Many conventional (nonoxide) superconductors with high transition temperatures have transitions that are accompanied by structural instabilities or structural transitions.[1] In some cases the structural transition may be arrested by the onset of superconductivity, but the structural instability remains. For conventional Bardeen-Cooper-Schrieffer (BCS) superconductors, the increase of the transition temperatures in materials near a structural instability is plausibly connected with their strong electron-phonon coupling. For the new oxide superconductors, the role of the lattice is uncertain, as evidenced by inconclusive isotope shifts.[2] Nevertheless, measurement of the sound velocities (and hence the elastic constants) is important because the elastic constants are a sensitive thermodynamic probe of the environment in which the electrons pair.

Single crystals of La_2CuO_4 were grown from a CuO flux, quenched, and later annealed at 650 K in N_2 for a short time and cooled to 300 K over 10 h. The ultrasound sample was oriented to within 1° of its principal axes via x rays. Neither x-ray nor polarized light scattering revealed any signs of twinning. Large twins in fractured samples are very apparent optically. However, if microtwins were present, we could not detect them using the methods available to us unless they were present in the entire sample. Thus partial twinning in our sample cannot be ruled out. Sample dimensions were $1.73\times1.76\times0.70$ mm^3, all ±0.01 mm, with the b axis parallel to the small dimension and normal to the Cu-O plane. The a and c axes were each oriented parallel to an edge, although they were not distinguished. After the N_2 anneal process, the measured density was 7.03 g/cm^3, compared to a theoretical density of 7.08 g/cm^3, suggesting reasonably good oxygen stoichiometry. The Néel temperature $T_N=305$ K for the ultrasound sample and $T_N=316$ K for the specific-heat sample, confirming the stoichiometry.[3]

Our relatively small single crystal would make pulse-echo measurements difficult. However, we were able to use a resonant method coupled with an elegant data analysis technique to deconvolute the resonant frequencies into elastic constants. Previous work on this problem has been done by Rayleigh,[4] Mindlin,[5] Demarest,[6] and Ohno.[7] The technique in its present form involves driving a sample with a continuous acoustic signal at a point of low symmetry, such as a corner. By sweeping the drive frequency, the normal modes of vibration are determined by the response of a second transducer at the corner diametrically opposite. A typical response trace is shown in Fig. 1, with a schematic of the experimental arrangement in the inset. If a sufficient number of resonances are measured, a numerical procedure can be used to extract all the elastic constants when the density and at least one sample dimension are known. This procedure is described in the Appendix. In our results, we have not corrected for the unknown but almost certainly anisotropic thermal expansion, but we expect it to be less

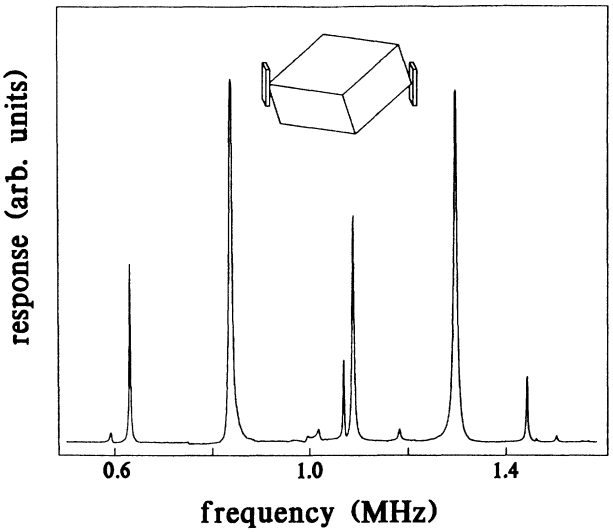

FIG. 1. A schematic diagram of the sample and cell used for the measurements is shown together with a typical room-temperature spectrum for the sample described in the text.

than 3×10^{-6} K^{-1} below 45 K.[8]

Table I contains a summary of the determination of the nine elastic constants (orthorhombic symmetry) at 310, 297, and 44 K. Because we did not distinguish the a and c axes, we have arbitrarily assigned the a axis to the 1 subscript and the c axis to the "2" subscript of the c_{ij}. The resonant frequencies themselves were determined using a fitting algorithm from raw data exhibiting quality factors (Q's) on the order of 1000. Because we have observed Q's on the order of 3×10^4 for fused silica, our sample (not the apparatus) must be responsible for the high dissipation. Unfortunately, we cannot rule out defect structures in general; thus the high dissipation may not be of intrinsic interest.

The bulk modulus B for our sample can be extracted from the c_{ij}. We obtain $B=1.126\times10^{12}$ dyn/cm$^2\pm0.5\%$ at 310 K, 1.125×10^{12} dyn/cm^2 at 297 K, and 1.138×10^{12} dyn/cm^2 at 44 K. Ledbetter *et al.*,[9] measured high-density powder samples and obtained very good agreement with our results. They found $B=1.145\times10^{12}$ dyn/cm^2 at room temperature, with a monotonic increase to 1.159×10^{12} dyn/cm^2 as the temperature was lowered. The average compressional wave speed (5.05 km/s) we derive from our data is in very good agreement with results on dense ceramics[10] (5.04 km/s). Because c_{66} is much stiffer than c_{44} or c_{55}, we find our average shear wave speed (3.26 km/s) to be substantially different than that for ceramics[10] (2.84 km/s). It is not unreasonable to expect the shear wave speed to be sensitive to details of the sintering process. Also included in Table I are the results of a molecular dynamics simulation carried out by Allan and Mackrodt.[11] Most significant is that the measured in-plane shear modulus c_{66} is much larger than their calculated value. The discrepancy demonstrates a fundamental failing of the expected force laws obtained from simple chemical considerations. This is not surprising in light of the predicted metallic nature of this material[12] from simple band-structure calculations. We do not know the reason for the discrepancies, although they may be a result of correlation effects that are not included in the simulations. The related antiferromagnetic[13] properties are also not included in the simulations, but magnetoelastic effects away from phase transitions are generally very weak compared to the differences shown in Table I.

In Figs. 2 and 3 we show sets of data representing the variation of some resonant frequencies with temperature. Above 70 K, we used chromel-constantan thermocouples with an absolute accuracy of 1 K; below 70 K we used both Pt resistance and gold-iron thermocouples, with an absolute accuracy of 0.1 K. Our temperature control was always better than the absolute errors in the thermometry, and the sample was surrounded by 1-bar He exchange gas. The frequencies plotted in Fig. 3 are almost exclusively dependent on c_{66}, whereas those plotted in Fig. 2 are primarily affected by changes in c_{11} and c_{22}. These data were not deconvoluted to obtain the variation in elastic constants because the deconvolution process produces additional scatter, making the trends harder to see. However, from our fits at 310, 297, and 44 K, we know the dependence of each frequency on each elastic constant at these temperatures. Between 25 and 54 K the dependence of frequencies on elastic constants is very close to the 44 K values. Note the features near 29 K in the compressional modes and the change in slope at 38 K for both compressional and shear.

Features at both temperatures are present in the heat capacity as well, as shown in Fig. 4. Heat-capacity measurements were made with an ac technique on samples from the same batch, but not the same fragment, as the

TABLE I. Elastic constants in 10^{12} dyn/cm^2. The last row is from Ref. 10, but we have taken the liberty of correcting an obvious error by a factor of 2 in several of their numbers. Note that data at 310 K was taken after the sample was removed and reinserted. We estimate our errors as follows. The rms frequency deviation in the fitting procedure was 6 kHz. We used a varying number of resonances (typically about 15) approximately uniformly distributed from 0.6 to 2.2 MHz. Thus the average fitting error is about 0.4%. Errors in sample dimensions and density were typically of order 1% as stated in the text. Thus our precision is 0.4% or better, and our absolute accuracy is about 1%.

T	c_{11}	c_{22}	c_{33}	c_{23}	c_{13}	c_{12}	c_{44}	c_{55}	c_{66}	Run number
310 K	1.722	1.716	2.000	0.732	0.728	0.892	0.652	0.658	0.971	2
297 K	1.719	1.712	2.000	0.731	0.727	0.904	0.656	0.658	0.968	1
44 K	1.688	1.668	2.000	0.728	0.714	1.000	0.705	0.660	1.036	1
	1.99	1.84	1.90	0.70	0.64	0.65	0.65	0.64	0.66	Ref. 10

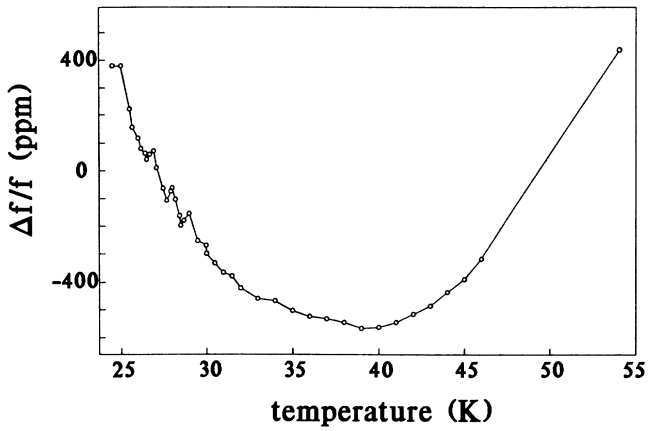

FIG. 2. The frequency of a resonance dependent primarily on c_{11} and c_{22} as a function of temperature. Temperature stability was 0.1 K and flexible 9 μm PVDF transducers were used. The frequency error bar is about 25 ppm.

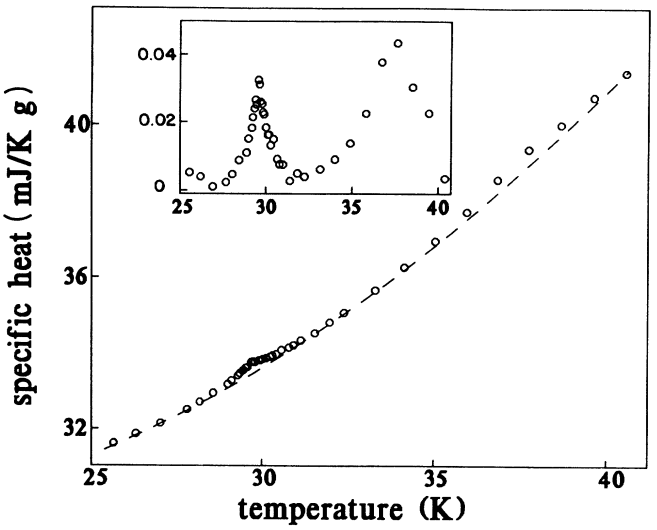

FIG. 4. Specific heat of intrinsic La_2CuO_4. The dashed line is the background, which we subtracted, and is chosen by a simple polynomial fit to the nonpeak data.

ultrasound sample and were annealed in a different run. The heat-capacity sample had a total mass of 2.2 mg ($1.5\times0.5\times0.5$ mm^3). Our calorimeter was made from thin (6×10^{-4} cm) Mylar foil cut into the shape of a cross with four arms (0.4×17 mm^2), and a central square 4×4 mm^2. This central square is the calorimeter. The four arms were mechanically and thermally anchored to a Cu ring that served at the thermal bath. Au-Ag and Ge-Au alloys were evaporated onto opposite faces of the square to be used as heater and thermometer, respectively. Ag film evaporated onto the four arms provided electrical contact for the heater and thermometer and also served as the weak thermal link. The La_2CuO_4 sample was attached to the calorimeter with 0.01 mg of silicone vacuum grease. The entire assembly was maintained in high vacuum. We achieved a precision of 0.1% in heat capacity after signal averaging. The operating frequency (0.05 Hz) was chosen to be between the internal and external equilibration rates for the calorimeter and sample. Addenda were about half of the total heat capacity and were determined in a separate run.

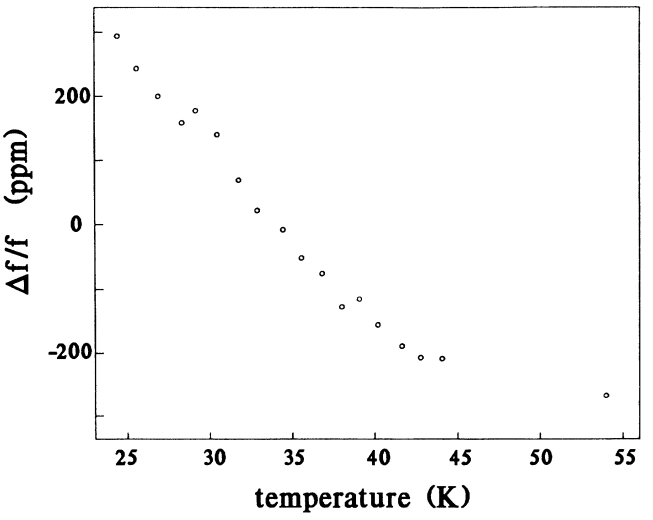

FIG. 3. The frequency of a resonance dependent only on c_{66} as a function of temperature. The temperature stability was 0.1 K, and rigid transducers were used. The frequency error bar is less than 25 ppm.

Two heat-capacity features, a relatively narrow one at 29.3 K and a broader one centered at 37.5 K, were observed. Note the correspondence of the broader heat-capacity peak (2.25×10^{-3} k_B/molecule) with the minimum in the compressional moduli at the same temperature. However, near 29 K we see only one feature in specific heat with an entropy of 7.57×10^{-4} k_B/molecule. Such behavior might be associated with some sort of structural defect or domain motion.[14] This feature does not appear to correspond with the small ultrasound features at the same temperature, perhaps because the samples were different.

In discussing the broader ultrasound minimum, we begin by emphasizing several key points. First, our sample is a single, at least partially untwinned, crystal at room temperature that shows no surface or bulk superconductivity when cooled. Second, the sound velocities for compressional waves normal to the Cu-O plane ($\sqrt{c_{33}/\rho}$) and for shear waves with both displacement vector and propagation vector in the Cu-O planes ($\sqrt{c_{66}/\rho}$) are significantly higher than for dense ceramics,[10] indicating strong anisotropy. Third, the system appears nearly tetragonal ($c_{44}=c_{55}$, $c_{11}=c_{22}$, etc.) at 297 K, but becomes increasingly orthorhombic as it is cooled. Taken together, these qualities establish that the interesting Cu-O plane produces anisotropic elastic effects, the in-plane anisotropies increase on cooling, and that elastic and specific-heat features appear in the nonsuperconductor at a temperature near T_c in the superconductor.

Others have seen unusual features near T_c in both superconducting and nonsuperconducting samples also. For example, Lang *et al.*[15] observe breaks in slope of the thermal expansion coefficient near 37 K in both La_2CuO_4 *and* fully superconducting $La_{1.85}Sr_{0.15}CuO_4$. Bhattacharya *et al.*[16] observe a strong stiffening of the shear modulus of superconducting ceramic $La_{1.8}Sr_{0.2}CuO_{4-y}$ below T_c that is similar to ours in the nonsuperconductor, but do not see the same broad local minimum in the compressional modulus. It thus appears that some of the observed thermodynamic and conductivity features present near T_c do not require the presence of superconductivity.

A minimum in the sound velocities is not typical of crystalline solids. It is common, however, in systems with low-frequency relaxation processes. Such systems include structural glasses[17] such as fused silica, which has a minimum in its sound velocities near 40 K caused by an attenuation peak there. Such effects also occur in ferromagnets,[14] where the activation of domain-wall motion strongly influences the temperature dependence of the elastic properties.

It is, therefore, compelling to look for an attenuation mechanism sensitive to temperature in the La_2CuO_4 system. One possibility is the oxygen sliding mode for which Cohen, Pickett, and Krakauer[18] have calculated the potential. They find the potential to be highly anharmonic, thereby providing a plausible link to attenuation. There is some direct evidence for anharmonic oxygen motions in neutron scattering measurements.[19,20] Should such an attenuation mechanism be responsible for the ultrasound results, then the attenuation will depend on frequency as well. This suggests that studies of the ultrasonic attenuation may clarify the processes we observe in the elastic moduli.

ACKNOWLEDGMENTS

The authors thank A. V. Granato, I. Rudnick, and S. A. Trugman for many useful suggestions. This work was performed at Los Alamos under the auspices of the United States Department of Energy and at the Pennsylvania State University under National Science Foundation (NSF) Grant Nos. DMR 8701 682, DMR 8701 651, DMR 8718 771, and under the U.S. Office of Naval Research (ONR).

APPENDIX

The determination of the resonant frequencies from the elastic constants is straightforward, and we begin by outlining this procedure. The method was introduced by Demarest[6] and expounded in detail by Ohno.[7] It is based on some remarkable attributes, consequences of Hamilton's principle, of the elastic Lagrangian integral

$$L=\int_V \mathcal{L}\, dV, \quad \text{where } \mathcal{L}=\tfrac{1}{2}\rho\omega^2 u_i u_i-\tfrac{1}{2}c_{ijkl}u_{i,j}u_{k,l}\ , \tag{1}$$

and where the domain of integration is the volume V of the sample, ω is the angular frequency, ρ is the density, u_i is the elastic displacement vector, $u_{i,j}$ are the strains, and the c_{ijkl} are the elastic constants. It can be easily demonstrated that the extrema of L, with respect to unrestricted variation of u_i's is realized for the u_i's that satisfy the elastic wave equation in V, and that satisfy the free-surface boundary conditions $n_j c_{ijkl}u_{k,l}=0$ on the boundary S, whose outer normal is n_j.

We exploit this fortunate fact by expanding the displacement vector in a complete set of orthonormal functions on V, viz.,

$$u_i=\sum_{l+m+n\le N} a_{ilmn}P_l(x/a)P_m(y/b)P_n(z/c)\ , \tag{2}$$

where the P_l's are Legendre polynomials, normalized on $(-1,1)$, and $2a,2b,2c$ are the sample dimensions. When (2) is substituted into (1), the integrals on x, y, and z can be done easily, and the result is an expression for L as a quadratic form in the expansion coefficients a_{ilmn}, which we can abbreviate as

$$L=\tfrac{1}{2}a^T(\rho\omega^2-\Gamma)a\ , \tag{3}$$

where Γ is a matrix linear in the c's, and a is the column vector $\{a_{ilmn}\}$, $i=1,2,3$, and $l+m+n\le N$. Extremizing (3) with respect to a_{ilmn} yields the eigenvalue equation

$$\Gamma a=\rho\omega^2 a\ . \tag{4}$$

Γ is symmetric with order $(N+1)(N+2)(N+3)/2$. N is chosen by compromising between precision and practicality. For $N=10$, this is an 858×858 matrix, but if we use a rectangular parallelepiped of a crystal having orthorhombic or higher symmetry, a tremendous simplification takes place. The matrix becomes block diagonal with eight blocks determined by symmetry and the largest block, for $N=10$, is 125×125. Thus it is straightforward to compute frequencies from elastic constants. The inverse problem is somewhat less so for many reasons.

The scheme we chose to accomplish the inversion includes the following steps.

(1) Estimate the elastic constants as closely as possible, if at all, from other sources.

(2) Form some function F of the differences between the observed and calculated frequencies that is a minimum when the two sets coincide. This may be as simple as a sum of squares, or there may be some reason to choose instead a sum of Gaussians or Lorentzians.

(3) F is clearly a highly nonlinear function of the elastic constants, density, and dimensions of the sample. One now uses some systematic scheme to search this multidimensional space to find the minimum of F. We have chosen to use *ZXCGS* (Ref. 20), which is an IMSL (Ref. 20) subroutine that uses a conjugate-gradient algorithm that converges on the minimum relatively quickly. The convergence criterion employed by *ZXCGS* is that the sum of the squares of the derivatives of F, with respect to the independent variables (which, in this case, are the c_{ijkl}'s and a,b,c), become less than some prescribed number.

Complicating factors include the following.

(a) Each resonance has a certain symmetry, and some have little or no motion of the corners perpendicular to

the transducer plane; hence they are ultrasonically invisible.

(b) The formation of F requires the assignment of each measured line to a calculated one in the ideal case, or, more realistically, at least the assumption that there can be a one-to-one correspondence if necessary.

(c) Therefore we need to assume that none of the lines have been missed (or at least we need to know roughly where the missing lines are), and we need to be relatively confident that no spurious lines are present, or at least to know which ones are spurious.

(d) There may be more than one minimum of F. The minima will always be shallover in some variables than in others, of course, which means that the shallow c's will be less accurately determined than the steeper ones. We have not yet done a detailed error analysis of the inversion scheme, so we do not have more than rough estimates of probable errors.

[1]R. L. Testardi, *Physical Acoustics: Principles and Methods,* edited by W. P. Mason and R. N. Thurston (Academic, New York, 1964), Vol. XIII.

[2]B. Batlogg, *et al.*, Phys. Rev. Lett. **59**, 912 (1987).

[3]S.-W. Cheong, J. D. Thompson, and Z. Fisk, Physica **158C**, 109 (1989).

[4]J. W. Strutt (Lord Rayleigh), *The Theory of Sound,* 2nd ed. (Dover, New York, 1945).

[5]R. D. Mindlin, J. Appl. Phys. **27**, 1462 (1956).

[6]H. H. Demarest, Jr., J. Acoust. Soc. Am. **49**, 768 (1971).

[7]I. Ohno, J. Phys. Earth **24**, 355 (1976).

[8]M. Lang *et al.*, Europhys. Lett. **4**, 1145 (1987).

[9]H. M. Ledbetter, S. A. Kim, C. E. Violet, and J. D. Thompson (unpublished).

[10]T. J. Kim *et al.*, J. Magn. Magn. Mater. **76&77**, 604 (1988).

[11]N. L. Allan and W. C. Mackrodt, Mater. Res. Soc. Symp. Proc. **99**, 797 (1988).

[12]R. V. Kasowski, W. Y. Hsu, and F. Herman, Solid State Commun. (to be published).

[13]S.-W. Cheong, Z. Fisk, and J. O. Willis *et al.*, Solid State Commun. **65**, 111 (1988).

[14]A. J. Heeger, O. Beckman, and A. M. Portis, Phys. Rev. **123**, 1652 (1961).

[15]J. D. Axe *et al.* (unpublished).

[16]S. Bhattacharya *et al.*, Phys. Rev. B **37**, 5901 (1988).

[17]S. Howklinger and M. V. Schickfus, *Amorphous Solids: Low Temperature Properties,* edited by W. A. Phillips (Springer-Verlag, New York, 1981).

[18]R. E. Cohen, W. E. Pickett, and H. Krakauer, Phys. Rev. Lett. **62**, 831 (1989); **60**, 817 (1989).

[19]T. Egami, W. Dmowski, and J. D. Jorgensen, Rev. Solid State Sci. **1**, 101 (1987).

[20]ZXCGS, from the International Mathematical and Statistical Libraries Inc., 7500 Belair Blvd., Houston, TX 77036.